Understanding the mechanisms behind high glacial productivity in the southern Brazilian margin

Rodrigo da C. Portilho-Ramos[1,2]. Tainã M. L. Pinho[3]; Cristiano M. Chiessi[3]; Cátia F. Barbosa[4]

[1]*MARUM - Center for Marine Environmental Sciences, University of Bremen, Leobener Strasse, 28359 Bremen, Germany.*
10 [2]*Institute of Geosciences, University of São Paulo, Rua do Lago 562, CEP05508-080, São Paulo, Brazil.*
[3]*School of Arts, Sciences and Humanities, University of São Paulo, Rua Arlindo Bettio 1000, CEP03828-000, São Paulo, Brazil.*
[4]*Departamento de Geoquímica, Universidade Federal Fluminense, Rua Outeiro São João Baptista S/N, CEP24020-141, Niterói, Rio de Janeiro, Brazil.*

Correspondence to: Portilho-Ramos, R.C (rcpramos@marum.de)

Abstract. This study explores the mechanisms behind the high glacial productivity in the southern Brazilian margin during the last 70 kyr. Therefore, we use planktonic foraminifera assemblage and subsurface
20 temperatures derived through the Modern Analogue Technique. We show that enhanced glacial productivity was driven by the synergy of two mechanisms operating in different seasons: (i) a enhanced productivity in the upwelling region during short austral summer events; and (ii) the persistent presence of the Plata Plume Water due to prolonged austral winter conditions. We suggest that the upwelling systems in the southern Brazilian margin were more productive during the last glacial period due to the enhanced Si supply for diatom
25 production through high-Si thermocline waters preformed in the Southern Ocean. We hypothesize that orbital forcing did not have a major influence on changes in upwelling during the last glacial period. However, the more frequent northward intrusions of the Plata Plume Water were modulated by austral winter insolation at 65°S through changes in the strength of alongshore SW-winds. After the Last Glacial Maximum, the reduced Si content of thermocline waters decreased upwelling productivity, while lower austral winter insolation
30 decreased the influence of the Plata Plume Water over the southern Brazilian margin, reducing regional productivity.

35

40

1. Introduction

Continental margins are regions of relatively high biological productivity and long-term carbon storage due to high nutrient flux (i.e., continental discharge and upwelling) and shallow seafloor depths (i.e., interception of sinking particulate organic matter) (Abrantes et al., 2016; Bianchi et al., 2005; Brandini et al., 2018; Ito et al., 2016; Wang et al., 2015). The high biological productivity and exportation of particulate organic carbon to the seafloor, the so-called "biological pump" (Turner, 2015), play a paramount role in removing CO_2 from the atmosphere (Bianchi et al.,2005; Muller-Karger et al., 2005). It is estimated that ca. 0.06Pg C yr^{-1} is buried in continental margins accounting for >40% of the carbon storage in the oceans (Muller-Karger et al., 2005). On the other hand, the upwelling of CO_2-rich thermocline waters along continental margins can release CO_2 to the atmosphere (Bianchi et al., 2005; Ito et al., 2016). Thus, continental margins have a great potential to modulate the drawdown and emission of atmospheric CO_2, influencing the Earth's climate system.

The southwestern Atlantic (southern Brazilian margin – SBM) is generally an oligotrophic area bathed by nutrient-poor, warm and salty tropical waters of the Brazil Current (BC) (Fig. 1). However, upwelling zones and riverine discharge inject nutrients into the photic zone (Brandini et al., 2018; Campos et al., 2000, 2013; Garcia and Garcia, 2008; Möller et al., 2008) resulting in confined areas and seasons with higher concentration of phyto-zooplankton biomass (Brandini et al., 2014; Rodrigues et al., 2014). During austral summer, upwelling zones are intensified due to the prevailing alongshore northeasterly winds and the cyclonic meanders of the BC induced by the interaction of the current with the morphology of the continental margin (Aguiar et al., 2014; Campos et al., 2000; Castelao et al., 2004). Winter conditions of vigorous alongshore SW-winds and a relatively weakened BC, allow the northward intrusion of low-salinity waters from the Plata River along the SBM (Garcia and Garcia, 2008; Möller et al., 2008). Both processes increase local productivity and lead to distinct changes in planktonic community (Brandini et al., 2014; Rodrigues et al., 2014), that are preserved in sea-floor sediments and can be used to reconstruct changes in productivity in the SBM over time (Gu et al., 2017; Lessa et al., 2017; Portilho-Ramos et al., 2015).

Previous paleoceanographic studies provide evidence for an extremely intense primary productivity in the SBM probably related to an upwelling system during part of Marine Isotope Stage 5 (~90 – 130 kyr) forced by strengthened NE-winds and BC (Lessa et al., 2017; Portilho-Ramos et al., 2015). During the last glacial period (Marine Isotope Stages 2-4, ~11.7 – 71 kyr), primary productivity weakened but was still significantly higher than the one occurring in the Holocene (Portilho-Ramos et al., 2015). It has been suggested that the upwelling systems of the SBM were reduced during the last glacial period, and may have been limited to short intervals of the austral summer due the prolonged winter-like conditions of prevalent alongshore SW-winds and frequent cold front passages (Portilho-Ramos et al., 2015). However, high abundance of eutrophic dinoflagellate cysts suggests increased primary productivity in the SBM during specific intervals of the last glacial period (Gu et al., 2017). These high productivity periods would be triggered by the input of local (i.e., Itajaí River) and remote riverine nutrient-rich freshwater (i.e., Plata River plume) (Gu et al., 2017). Additionally, a recent study proposed that the periods of expansion and contraction of the upwelling zones of the SBM are modulated by eccentricity (Lessa et al., 2017), providing yet another mechanisms to explain the evolution of primary productivity in the SBM. In summary, these studies show that different oceanographic mechanisms may have triggered high primary productivity in the SBM over

time. These mechanisms are, however, poorly understood.

Here we used records of planktonic foraminifera assemblage and associated subsurface temperature reconstructions derived by the Modern Analogue Technique (MAT) from piston core JPC-17 (27°52.73'S, 46°55.25'W) to understand the paleoceanographic processes controlling changes in biological productivity in the SBM over the last 70 kyr. The comparison of our results to previously published records from the SBM allowed us to recognize two different mechanisms modulating past productivity changes over the last glacial-interglacial cycle.

2. Regional setting

The SBM is an oligotrophic margin under the influence of warm ($\geq 25^{\circ}$C) and salty (≥ 35psu) Tropical Water that flows southward within the BC (Fig. 1). Interactions of the BC with the morphology of the margin (i.e. changes in the orientation of the margin and the presence of a barrier represented by the Abrolhos bank), besides other oceanographic processes, generates cyclonic meanders and eddies that bring cold ($\leq 20^{\circ}$C) and nutrient-rich thermocline waters (South Atlantic Central Waters (SACW) to shallower depths where they are subjected to alongshore NE-winds (Aguiar et al., 2014; Campos et al., 2000; Castelao et al., 2004; Rodrigues and Lorenzzetti, 2001). Once over the shelf, wind stress and the Ekman dynamics brings the SACW to the surface creating mature upwelling zones in the SBM (Aguiar et al., 2014; Castelao et al., 2004). These processes boost biological productivity in specific portions of the SBM such as off Vitória ($\sim18^{\circ}$S), Cabo Frio (22°–23°S) and Cape Santa Marta (27°–29°S) during the austral summer (Fig. 1). Marine sediment core JPC-17 investigated in this study was collected off Cape Santa Marta (Fig. 1).

In the vicinities of Cape Santa Marta, local productivity is also enhanced by the injection of nutrients from freshwater discharge of local (i.e. Itajaí River) and remote (i.e. Plata River and Patos/Mirim Lagoon complex) sources (Garcia and Garcia, 2008; Möller et al., 2008). During the summer (Fig. 1A), the upwelling favorable NE-winds and the strong BC block the northward penetration of the PPW (at ca. 32°S) (Campos et al. 2013; Möller et al. 2008). During austral winter (Fig. 1B), the weakened BC and the prevailing alongshore SW-winds increase the northward intrusion (up to ca. 27°S) of the nutrient-rich, cold ($\leq 18^{\circ}$C) and low salinity (≤ 33.5psu) Plata Plume Water (PPW) (Campos et al. 2013; Möller et al. 2008).

Both upwelling and freshwater inject large amounts of nutrients into the oligotrophic SBM, modulating seasonally the biological productivity as well as plankton community in the region (Garcia and Garcia, 2008; Rodrigues et al., 2014). In the vicinities of the Cape Santa Marta, diatoms are the dominant group of phytoplankton, accounting for 29–90% of phytoplankton and 31–90% of the carbon biomass during the summer upwelling, while dinoflagellates dominates the phytoplankton during the winter intrusion of the PPW (Brandini et al., 2014).

3. Material and methods

Piston core KNR159-5-17JPC (27°52,73'S and 46°55,25'W) recovered 15 m from which the uppermost 340 cm were investigated in this study. The core was raised from 1627 m water depth during R/V KNORR cruise 159-5 from Woods Hole Oceanographic Institution (WHOI, USA) (Fig. 1). The upper 350 cm

120   of the core consist in dark gray carbonate limestone. This section was sampled continuously every 10 cm and
2 g of sediment per sample were washed in 62 µm sieves.

3.1. Planktonic foraminifera assemblage

125   Planktonic foraminifera from core JPC-17 were dry picked from >150 µm size fraction and
quantified in relative abundances from splits containing more than 300 specimens per sample. The taxonomy
was based on Stainforth et al., (1975). We assumed the effect of dissolution in our planktonic foraminiferal
faunal composition to be negligible since core JPC-17 was collected at 1627 m water depth, well above the
modern and glacial lysocline (Volbers and Henrich, 2004). Here we do not distinguish between
130   *Globigerinoides ruber* white and pink variety, and also counted *Globigerinoides sacculifer* and
Globigerinoides trilobus together as *G. sacculifer* since they are genetically the same species (André et al.,
2012). Considering the taxonomic ambiguity in distinguishing the small-sized (*i.e.* ≤250 µm) specimens of
Globigerinella calida and *Globigerinella siphonifera* (Vargas et al., 2002) we counted them together as *G.
siphonifera*.

135

3.2. Subsurface temperature reconstruction

We reconstructed subsurface temperatures at 100 m water depth using the modern analog technique
(MAT) following Portilho-Ramos et al. (2015). The MAT was performed on the software C2 (Juggins, 2007)
and the basic assumption is that temperature of ambient seawater the primary control of foraminiferal
140   assemblage. The planktonic foraminiferal calibration dataset used here comprises 301 surface samples from
the Atlantic Ocean between 10°N and 60°S from the MARGO Project (Kucera et al., 2005a) and is available
at PANGAEA (http://epic.awi.de/30068/). The modern annual temperature values at 100m water depths from
WOA 2009 (Locarnini et al., 2010) were extracted and used to calibrate the MAT. For the MAT transfer
function, the squared chord distance was applied as similarity measure. Additionally, when reconstruction
145   results were evaluated, the weighted mean of the best 10 modern analogs was used (Kucera et al., 2005b).
Using the leave-one-out cross-validation method, the root mean square error of prediction (RMSEP) of the
transfer function was calculated as 1.5 °C (R^2 = 0.9).

3.3. Age model

150   An age model for core JPC-17 has been previously published on the basis of calibrated radiocarbon
AMS ^{14}C ages, δ^{18}O in both planktonic and benthic foraminifera as well as regional planktonic foraminifera
biostratigraphy (Portilho-Ramos et al., 2014a; Tessin and Lund, 2013). Reversals in radiocarbon ages from
ca. 16 to 21 calibrated kiloannum before present (i.e. 1950 AD) (cal ka BP) where detected by Tessin and
Lund (2013). Tessin and Lund (2013) excluded four radiocarbon ages (i.e. 50, 54, 58 and 82 cm core depth)
155   out of 17 dated samples from core JPC-17 because of reversals (Table 1). Since the radiocarbon age obtained
at 56 cm from Portilho-Ramos et al. (2014a) is placed within this interval and also seems to be reversed, we
decide to exclude this radiocarbon age as well, on top of the four ages excluded by Tessin and Lund (2013).
Here we recalibrated the remaining 12 AMS ^{14}C ages from Tessin and Lund (2013) and Portilho-Ramos et al
(2014a) using the Marine13 calibration curve (Stuiver and Reimer, 1993). All AMS ^{14}C ages were corrected

160 for a reservoir age using ΔR of 7±59 yr (Angulo et al., 2007) and translated into calendar ages (Table 1) using the Calib 7.1 software (Stuiver and Reimer, 1993). For the core section that extrapolates the radiocarbon range, additional tie-points were obtained by confronting benthic foraminifera δ^{18}O records from JPC-17 to benthic δ^{18}O of nearby core GL-1090 (Santos et al., 2017) (Fig. 1) and to the intermediate-depth South Atlantic benthic δ^{18}O stack LS16 (Lisiecki and Stern, 2016) using the Analyseries 2.0.5.2 software (Paillard

165 et al., 1996) (Fig. 2). The benthic δ^{18}O curve from JPC-17 is a combination of published *Cibicidoides* spp. (Tessin and Lund, 2013) and unpublished *Cibicidoides* spp. data δ^{18}O provided by WHOI (Fig. 2). The latest follow the methodology applied in (Curry and Oppo, 2005). All radiocarbon and δ^{18}O tie-points are shown in Table 1. The new age model was obtained by linear interpolation of the radiocarbon and δ^{18}O tie-points. The chronology of core JPC-17 was additionally verified and supported by planktonic foraminifera

170 biostratigraphy (Ericson and Wollin, 1968; Portilho-Ramos et al., 2014b), where the presence of *Globorotalia menardii* and the low abundance of *Globorotalia inflata* indicate Biozone Z (Holocene), while the absence of *G. menardii* and the high abundance of *G. inflata* characterize the glacial Biozone Y (last glacial period) (Fig. 2).

175 **4. Results**

In contrast to a previous chronology (Portilho-Ramos et al., 2014a), the new age model for the upper 350 cm of core JPC-17 spans the last ca. 70 cal ka BP (Fig. 2). The benthic oxygen isotope records from core JPC-17 display a clear glacial-interglacial pattern, comparable to the benthic δ^{18}O record of nearby core GL-1090 as well as that of the intermediate-depth South Atlantic benthic δ^{18}O stack LS16 (Lisiecki and Stern,

180 2016) (Fig. 2).

Planktonic foraminifera assemblage is composed by 28 species and subspecies. The following six species accounted for more than 70% of total planktonic assemblage: *G. ruber* (39%); *Globigerina glutinata* (13%); *G. bulloides* (11.2%); *G. inflata* (8.8%); *G. sacculifer* (5%); and *G. siphonifera* (2.5%). The abundance of *G. menardii* (0.7%), *Pulleniatina obliquiloculata* (0.3%), *Orbulina universa* (0.3%),

185 *Globorotalia crassaformis* (0.3%), *Neogloboquadrina dutertrei* (5.5%) and *Globorotalia truncatulinoides* (3.9%) was published in Portilho-Ramos et al (2014).

In general, the distribution of the most abundant species follows the glacial-interglacial pattern over the last 70 kyr (Fig. 3). The abundance of the non-spinose species *G. bulloides* and *G. inflata* were higher during the last glacial period (mean of 12% and 9.6%, respectively) and lower during the Holocene (mean of

190 4.6% and ~2%, respectively) (Fig. 3A, 3B, respectively). In contrast, the abundance of spinose species displayed the opposite behavior. The abundance of *G. ruber* ranged from 25 to 50% (mean of 39%) during the glacial and increased after 40 cal ka BP towards the Holocene (mean of 47) (Fig. 3C). The abundance of *G. sacculifer* and *G. siphonifera* display similar patterns (Fig. 3D, E, respectively), and ranged between 1.6– 10.4% and 0–7.6% (respectively), with higher abundance during the postglacial interval (mean of 7.5 and

195 6.9%, respectively).

The temperature at 100 m-water depth derived from MAT ranged from 17.5 to 23°C over the last 70 kyr with lower temperatures recorded during the glacial (17.5– 20.3°C) in comparison to the Holocene (~23°C) (Fig. 3F). A pronounced warming trend is observed after 40 cal ka BP toward the Holocene.

5. Discussion

Planktonic foraminifera *G. bulloides* is a non-spinose surface-dwelling species generally inhabiting regions of cold and high phytoplankton biomass typically associated with upwelling zones (Lessa et al., 2014; Mohtadi et al., 2007; Sautter and Thunell, 1991). Thus, high abundances of *G. bulloides* in marine sediments from regions potentially affected by upwelling has been widely used as an upwelling indicator (Godad et al., 2011; Peeters et al., 2002), including the SBM upwelling zones (Lessa et al., 2017; Portilho-Ramos et al., 2015). The last glacial abundance of *G. bulloides* in core JPC-17 (8–18%) (Fig. 3A) closely matches those found in surface sediments from the Cabo Frio upwelling (10−20%) (Lessa et al., 2014), suggesting the occurrence of a sustained upwelling off Cape Santa Marta in the SBM. It also closely matches glacial records from cores collected further north at the SBM like GL-75 (21°83`S; 40°01`W) (Portilho-Ramos et al., 2015), GL-77 (21º12'S; 40º02'W) (Petró et al., 2016) and SAN 76 (24°26′S; 42°17′W) (Toledo et al., 2007), where *G. bulloides* ranged between 8%–17%, suggesting widespread cooling and elevated productivity at the SBM during the last glacial period relative to the modern oligotrophic conditions (Fig. 4A, B). During the last glacial period, the reduced abundance of non-upwelling species *G. ruber* (25–50%) and other warm and oligotrophic symbiont-bearing species like *G. sacculifer* (2.1–10.4%) and *G. siphonifera* (0.3%–4.3%) (Fig. 3) support the occurrence of cold-productive conditions promoted by upwelling. Simultaneously, lower temperatures at 100 m water depth ($\leq 20^{o}$C) suggest that SACW may have been frequently located in the photic zone. The isotherm of 20°C is used to track the boundary between Tropical Water and SACW (Castelao et al., 2004), and has been used as a proxy for the presence of SACW in the photic zone in the past (Portilho-Ramos et al., 2015; Lessa et al., 2017). It should be highlighted that a relative warming of thermocline waters observed between 20 – 35 cal ka BP may be related to heat accumulation in the western South Atlantic associated to the glacial reduced mode of the Atlantic meridional overturning circulation (Santos et al., 2017).

Enhanced glacial productivity in the SBM was recently reported by a 74 kyr-long record of dinoflagellate cysts from adjacent core GeoB2107-3 (27°17'S; 46°45"W) (Gu et al., 2007). The authors provide evidences for increased eutrophic conditions associated to more frequent northward intrusions of the PPW (Fig. 4D) (Gu et al., 2017). However, *G. bulloides* is virtually absent in surface sediments deposited under the influence of the PPW to the north from the Brazil-Malvinas Confluence (Chiessi et al., 2007). Thus, more frequent northward penetrations of the PPW in our study site is unlikely to explain the enhanced glacial abundance of *G. bulloides*. In addition, the abundance of the eutrophic environmental dinocysts and *G. bulloides* show different behavior along the last glacial period (Fig. 4A, D). The dinocysts increased in abundance between 54–74 cal ka BP and 14–40 cal ka BP, suggesting increased productivity related to frequent northward intrusions of the PPW, while the opposite is observed between 40–54 cal ka BP (Fig. 4D), suggesting reduced influence of the PPW and relatively low productivity (Gu et al., 2017). In contrast, the abundance of the *G. bulloides* remained relatively high during the entire glacial with a decrease trend after 30 cal ka BP toward the Holocene (Figs. 3A, 4B). Furthermore, enhanced abundance of *G. bulloides* during the last glacial period is also observed as far north as 21ºS (i.e. core GL-75) (Fig. 4A) (Portilho-Ramos et al., 2015), which is unlikely be explained by continuous presence of the PPW (Möller et al., 2008). In summary, enhanced abundance of *G. bulloides* indicates that upwelling systems in the SBM were markedly active during the last glacial period and its mismatch with dinoflagellate cysts assemblages suggests that both taxa

240   recorded different seasonal oceanographic processes responsible for boosting primary productivity in the
        SBM: the Cape Santa Marta upwelling and the more frequent northward intrusions of the PPW.

5.1. Modern and past seasonal productivity processes in the SBM

        Modern surface productivity in the SBM is seasonally modulated by two different processes that
245   inject nutrients in the photic zone: (i) austral summer coastal and shelf-break upwelling (Campos et al., 2013);
        and (ii) austral winter northward intrusions of the PPW (Garcia and Garcia, 2008; Möller et al., 2008). During
        austral summer upwelling events, diatoms are the dominant group of the phytoplankton, accounting for 29–
        90% of phytoplankton density and 31–90% of the carbon biomass (Brandini et al., 2014). On the other hand,
        dinoflagellate is the dominant group during the austral winter associated to northward intrusions of the PPW
250   (Brandini et al., 2014). We suggest that both taxa reveal different seasonal conditions during the last glacial
        period, with *G. bulloides* recording upwelling events during austral summer and dinoflagellate recording
        northward intrusions of the PPW during austral winter.

        Prolonged winter-like conditions of prevalent alongshore SW-winds and frequent cold front passages
        during the last glacial period may have limited the SBM upwelling systems to a short period of austral
255   summer-like conditions, as suggested by Portilho-Ramos et al. (2015). Furthermore, increased continental
        runoff (i.e. Itajaí River, Plata River and Patos/Mirim Lagoon complex) associated to enhanced precipitation
        over SE South America (Cruz et al., 2005; Wang et al., 2007) as well as a vigorous alongshore SW-winds
        were favorable to the northward penetration of the PPW. These conditions increased the abundance of
        eutrophic environmental dinocysts in the SBM during the glacial (Gu et al., 2017). The lower sea level
260   (Waelbroeck et al., 2002) may have caused offshore displacement of the PPW over to our core site location
        (Lantzsch et al., 2014).

        Importantly, our reconstructed temperature at 100 m water depth indicates that SACW may have
        reached the photic zone during the last glacial period (Fig. 3F). Modern hydrographic data and model
        simulations show that shelf-break upwelling in the SBM induced by the interaction of the BC with bottom
265   topography occurs year-long but is modulated by seasonal alongshore-wind direction (Brandini et al., 2018;
        Campos et al., 2013). Thus, a prolonged presence of the low salinity PPW in the region may have increased
        the upper water stratification and suppressed the surfacing of SACW, favoring the proliferation of eutrophic
        environmental dinocysts. In contrast, during short austral summer periods, the strengthening of both the
        alongshore NE-winds and the BC hampered the northward PPW migration, inducing the upwelling of SACW
270   and creating favorable conditions to the proliferation of *G. bulloides*. Owing to the low resolution of core
        JPC-17, we cannot rule out an anthiphase between the *G. bulloides* (i.e. core JPC-17) and the eutrophic
        environmental dinocyst (i.e., coe GeoB2107-3) records that would assign the SW-winds and the associated
        northward penetration of PPW a key role on controlling the upwelling zones in the SBM during the last
        glacial period.

275

5.2. Orbital forcing of SBM upwelling systems

        A recent study proposed orbitally forced changes in insolation (eccentricity) as a major mechanism
        modulating the intensification/deintensification as well as the expansion/contraction dynamics of the SBM
        upwelling zones (Lessa et al., 2017). In accordance to these authors, eccentricity maximum (≥ 0.03) during

MIS5 would have altered the seasonality of the wind regime by controlling the amplitude of austral summer and winter insolation and the South Atlantic subtropical high-pressure position. Thus, prolonged NE-winds during austral summer promoted intensification and expansion (from 24°S to 28°S) of the SE-Brazil upwelling systems during MIS5. On the other hand, eccentricity minimum (≤ 0.02) during the Holocene would result in weak NE-winds and deintensifying and contracting these upwelling systems in comparison to MIS5 (Lessa et al., 2017).

However, the orbital mechanism proposed by Lessa et al. (2017) do not explain the intensified/expanded upwelling in the SBM during the last glacial period, since eccentricity was ≤0.02 during the entire interval (Fig. 4C). Interestingly, the eutrophic environmental dinocyst record from core GeoB2107-3 matches very well austral winter (June) insolation at 65°S over the last 70 kyr (Fig. 4D), highlighting the close connection between dinocyst abundance and winter conditions through vigorous alongshore SW-winds and increased presence of the PPW in our core site. Periods of increased austral winter insolation at 65°S may have steeped the thermal gradient between the high and mid latitudes in the Atlantic sector of the Southern Ocean, intensifying the alongshore SW-wind system and the northward incursion of PPW, thereby boosting the eutrophic environmental dinocyst productivity in the SBM.

5.3. The silicic acid leakage hypothesis (SALH)

In sections 5.1 and 5.2, we showed that *G. bulloides* and eutrophic environmental dinocysts record different seasonal productivity processes in the SMB. While austral winter productivity events were triggered by the more frequent northward intrusions of the PPW, it is not clear what could explain the occurrence of austral summer productivity events related to upwelling in the SBM.

We suggest that, rather than intense as observed during interglacial MIS5 (Lessa et al., 2017; Portilho-Ramos et al., 2015), upwelling in the SBM may have been more productive due to the increased silicic acid content supplied by the glacial SACW. Several paleorecords and model experiments addressed the hypothesis of increased export of dissolved silicic acid preformed in the Southern Ocean that have fueled primary diatom productivity in low latitude upwelling zones and continental margins during the last glacial period, the so called "silicic acid leakage hypothesis" (SALH) (Bradtmiller et al., 2007; DeMaster, 2002; Matsumoto et al., 2014; Sarmiento et al., 2004). The SALH postulates that during glacial periods, imposed sea ice around Antarctica displaced the zone of high diatom production to the North of the Antarctic Polar Front (APF), where thermocline waters (i.e. Subantarctic Mode Water, a precursor of SACW) are formed (Abelmann et al., 2015; Bradtmiller et al., 2007; Sarmiento et al., 2004). Thus, (unused) high-Si waters were exported from the Southern Ocean to the low latitude world ocean, where diatom production increased at the expense of other types of phytoplankton (Bradtmiller et al., 2007; Sarmiento et al., 2004).

Currently, diatoms dominate the phytoplankton in the SBM during austral summer SACW upwelling (Brandini et al., 2014) and are an important component of the diet of the symbiotic-barren *G. bulloides*, which can alternatively feed on zooplankton (i.e., copepods) (Sautter and Thunell, 1991; Schiebel and Hemleben, 2017; Thunell and Sautter, 1992). Within age model uncertainties (including also the radiocarbon reversals in our core) and considering the different temporal resolution of the records, the glacial high abundance of *G. bulloides* in core JPC-17 matches well with high biogenic Opal% in sediments north of the APF Front as recorded in core RC13-254 (Atlantic sector) (Mortlock et al., 1991) (Fig. 4B, F). It is noteworthy that SACW

320 also receives contributions from the Indian Ocean through the Agulhas Leakage (warm water route; Donners and Drijfhout, 2004), where the production of opal (north of the APF) and export of silicic acid remained high over the entire last glaciation (Dezileau et al., 2003). We suggest that *G. bulloides* in the SBM may have benefited the silicic acid-induced diatom blooms by directly feeding diatoms and/or indirectly by preying other zooplankton that also feed on diatoms. Thus, the increased abundance of *G. bulloides* in the SBM

325 during the last glacial period was related to upwelling-driven high productivity during short austral summer periods, as previously suggested in Portilho-Ramos et al. (2015). In contrast, prolonged austral winter conditions with vigorous alongshore SW-winds as well as increased precipitation over SE South America (Cruz et al., 2005; Wang et al., 2007) increased the northward penetration of the PPW leading to enhanced eutrophic environmental dinocyst productivity during the last glaciation (Gu et al., 2017). Taken together,

330 both processes may have boosted biological primary productivity along the year during the last glacial period. This is supported by enhanced abundance of deep-dwelling herbivorous planktonic foraminifera species *Globorotalia inflata* (Schiebel and Hemleben, 2017) that calcifies between 200 and 400 m water depth (Chiessi et al., 2007) and would have benefited by grazing the increased amount of sinking organic particles.

335 **5.4. Post-glacial conditions**

After the Last Glacial Maximum, the abundance of *G. bulloides* and eutrophic environmental dinocycts decrease until the onset of the Holocene, suggesting decreased regional productivity and more oligotrophic conditions in comparison to the last glacial period (Fig. 4B, D). Oligotrophic conditions is supported by increased abundance of tropical symbiont-bearing species *G. ruber* (37%–52%), *G. sacculifer*

340 (6% – 8.8%) and *G. siphonifera* (6.3% – 7.5%) (Fig. 3). The low abundance of *G. inflata* also suggests oligotrophic conditions during the Holocene (Fig. 3B). Despite the favorable conditions for upwelling in the SBM during the Holocene (i.e. occurrence of alongshore NE-winds and a strong BC) (Lessa et al., 2017; Portilho-Ramos et al., 2015), upwelling productivity may have been hampered by the reduced export of pre-formed silicic acid through SACW (Fig. 4E, F). Indeed, the retraction of Antarctic sea ice displaced the zone

345 of enhanced biogenic opal production to the south of the APF, retaining the excess of silicic acid and opal burial in the Southern Ocean (Bradtmiller et al., 2007; Sarmiento et al., 2004) as evidenced by increased Holocene Opal% to the South of the APF core RC13-259 (Fig. 4F; Mortlock et al., 1991). In addition, low austral winter insolation at 65°S and reduced sea ice may have decrease the thermal gradient between the high and mid latitudes in the Atlantic sector of the Southern Ocean and consequently weakened the alongshore

350 SW-winds in the SBM, inhibiting the northward intrusions of the PPW. Simultaneously, the high sea level stand modified the SBM morphology increasing the width of the southern Brazilian shelf and, displacing the core of the upwelling zone to the inner shelf off Cape Santa Marta where it is controlled by local factors such as coastal wind system (Campos et al., 2013; Möller et al., 2008). The high temperatures at 100 m water depth from core JPC-17 (Fig. 3F) support this hypothesis, suggesting that the SACW was not frequently in

355 the photic zone at the core location.

6. Conclusions

In this study we used planktonic foraminifera assemblage and associated 100 m water depth temperatures to discuss changes in productivity in the southern Brazilian margin over the last 70 kyr. The

enhanced abundance of upwelling indicator *Globigerina bulloides* (12–16%) together with the reduced abundance of oligotrophic species and subsurface temperatures lower than 20°C suggest the occurrence of upwelling off Cape Santa Marta during the last glacial period. We suggested that rather than intense, upwelling might have been more productive, due the increased silicic acid export from the Southern Ocean through South Atlantic Central Water. Our results show that orbital forcing did not have a major influence on changes in upwelling during the last glacial period. We further show that more frequent northward intrusions of Plata Plume Water modulated by austral winter insolation at 65°S through enhanced alongshore SW–winds boosted austral winter productivity at the SBM. Thus, a productive upwelling during short austral summer events and the prolonged presence of Plata Plume Water during austral winter enhanced the biological productivity year-round in the SBM during the last glacial period relative to modern conditions. After the Last Glacial Maximum, low silicic acid content in thermocline waters decreased the productivity of the upwelling, while lower austral winter insolation at 65°S and associated weakened SW-winds reduced the presence of the Plata Plume Water in the SBM. In addition, last deglaciation sea level rise may have modified the geomorphology of the SBM limiting the upwelling system to the coast, southern to Cape Santa Marta.

Acknowledgments. We are grateful to Delia Oppo and William B. Curry from Woods Hole Oceanographic Institute, United States, for providing the oxygen isotope data from core JPC-17 used here. R.C.P.-R. thanks PNPD scholarship from CAPES. T.M.L.P. thanks PIBIC scholarship from CNPq (2017-482). C.M.C. acknowledges the financial support from FAPESP (grant 2012/17517-3), CAPES (grants 1976/2014 and 564/2015) and CNPq (grants 302607/2016-1 and 422255/2016-5).

Data availability. The data reported here will be archived in in the World Data Center PANGAEA (www.pangaea.de).

Author Contributions

R.C.P.-R. and C.M.C. designed the study. R.C.P.-R. and T.M.L.P. analyzed planktonic foraminifera assemblage. R.C.P.-R and C.M.C. wrote the manuscript. R.C.P.-R. performed the Modern Analogue Technique. R.C.P.-R. and C.F.B performed age modeling. All authors contributed to the interpretation of the data.

Competing interests. The authors declare that they have no conflict of interest.

7. References

Abelmann, A., Gersonde, R., Knorr, G., Zhang, X., Chapligin, B., Maier, E., Esper, O., Friedrichsen, H., Lohmann, G., Meyer, H. and Tiedemann, R.: The seasonal sea-ice zone in the glacial Southern Ocean as a carbon sink, Nature Communications, 6(1), 8136, doi:10.1038/ncomms9136, 2015.

Abrantes, F., Cermeno, P., Lopes, C., Romero, O., Matos, L., Van Iperen, J., Rufino, M. and Magalhães, V.: Diatoms Si uptake capacity drives carbon export in coastal upwelling systems, Biogeosciences, 13(14), 4099–4109, doi:10.5194/bg-13-4099-2016, 2016.

Aguiar, A. L., Cirano, M., Pereira, J. and Marta-Almeida, M.: Upwelling processes along a western boundary current in the Abrolhos-Campos region of Brazil, Continental Shelf Research, 85, 42–59, doi:10.1016/j.csr.2014.04.013, 2014.

André, A., Weiner, A., Quillévéré, F., Aurahs, R., Morard, R., Douady, C. J., de Garidel-Thoron, T., Escarguel, G., de Vargas, C. and Kucera, M.: The cryptic and the apparent reversed: lack of genetic differentiation within the morphologically diverse plexus of the planktonic foraminifer *Globigerinoides sacculifer*, Paleobiology, 39(1), 21–39, doi:10.1666/0094-8373-39.1.21, 2012.

Angulo, R. J., Reimer, P. J., Souza, M. C. de, Scheel-Ybert, R., Tenório, M. C., Disaró, S. T. and Gaspar, M. D.: A tentative determination of upwelling influence on the paleosurficial marine water reservoir effect in southeastern Brazil., Radiocarbon, 49(3), 1255–1259, 2007.

Bianchi, A., Bianucci, L., Piola, A. R., Pino, D. R. Schloss, I., Poisson, A. and Balestrini, C.F., Vertical stratification and air-sea CO_2 fluxes in the Patagonian shelf, Journal of Geophysical Research, 110(C7), C07003, doi:10.1029/2004JC002488, 2005.

Bradtmiller, L. I., Anderson, R. F., Fleisher, M. Q. and Burckle, L. H.: Opal burial in the equatorial Atlantic Ocean over the last 30 ka: Implications for glacial-interglacial changes in the ocean silicon cycle, Paleoceanography, 22(4), PA4216, doi:10.1029/2007PA001443, 2007.

Brandini, F. P., Nogueira, M., Simião, M., Codina, J. C.U. and Noernberg, M. A.,: Deep chlorophyll maximum and plankton community response to oceanic bottom intrusions on the continental shelf in the South Brazilian Bight, Continental Shelf Research, 89, 61–75, doi:10.1016/J.CSR.2013.08.002, 2014.

Brandini, F. P., Tura, P. M. and Santos, P. P. G. M.: Ecosystem responses to biogeochemical fronts in the South Brazil Bight, Progress in Oceanography, 164(April), 52–62, doi:10.1016/J.POCEAN.2018.04.012, 2018.

Campos, E. J. D., Velhote, D. and Da Silveira, I. C. A.: Shelf break upwelling driven by Brazil current cyclonic meanders, Geophysical Research Letters, 27(6), 751–754, doi:10.1029/1999GL010502, 2000.

Campos, P. C., Möller, O. O., Piola, A. R. and Palma, E. D.: Seasonal variability and coastal upwelling near Cape Santa Marta (Brazil), Journal of Geophysical Research: Oceans, 118(3), 1420–1433, doi:10.1002/jgrc.20131, 2013.

Castelao, R. M., Campos, E. J. D. and Miller, J. L.: A Modelling Study of Coastal Upwelling Driven by Wind and Meanders of the Brazil Current, Journal of Coastal Research, 203, 662–671, doi:10.2112/1551-5036(2004)20[662:AMSOCU]2.0.CO;2, 2004.

Chiessi, C. M., Ulrich, S., Mulitza, S., Pätzold, J. and Wefer, G.: Signature of the Brazil-Malvinas Confluence (Argentine Basin) in the isotopic composition of planktonic foraminifera from surface sediments, Marine Micropaleontology, 64(1-2), 52–66, doi:10.1016/j.marmicro.2007.02.002, 2007.

Cruz, F. W., Burns, S. J., Karmann, I., Sharp, W. D., Vuille, M., Cardoso, A. O., Ferrari, J. A., Dias, P. L. S. and Viana, O.: Insolation-driven changes in atmospheric circulation over the past 116,000 years in subtropical Brazil., Nature, 434(7029), 63–6, doi:10.1038/nature03365, 2005.

Curry, W. B. and Oppo, D. W.: Glacial water mass geometry and the distribution of $\delta^{13}C$ of ΣCO_2 in the western Atlantic Ocean, Paleoceanography, 20(1), n/a–n/a, doi:10.1029/2004PA001021, 2005.

440   DeMaster, D. J.: The accumulation and cycling of biogenic silica in the Southern Ocean: Revisiting the marine silica budget, Deep-Sea Research Part II: Topical Studies in Oceanography, 49(16), 3155–3167, doi:10.1016/S0967-0645(02)00076-0, 2002.

Dezileau, L., Reyss, J. L. and Lemoine, F.: Late Quaternary changes in biogenic opal fluxes in the Southern Indian Ocean, Marine Geology, 202(3-4), 143–158, doi:10.1016/S0025-3227(03)00283-4, 2003.

445   Donners, J. and Drijfhout, S. S.: The Lagrangian View of South Atlantic Interocean Exchange in a Global Ocean Model Compared with Inverse Model Results, Journal of Physical Oceanography, 34(5), 1019–1035, doi:10.1175/1520-0485(2004)034<1019:TLVOSA>2.0.CO;2, 2004.

Ericson, D. B. and Wollin, G.: Pleistocene Climates and Chronology in Deep-Sea Sediments, Science, 162(3859), 1227–1234, doi:10.1126/science.162.3859.1227, 1968.

450   Garcia, C. A. E. and Garcia, V. M. T.: Variability of chlorophyll-a from ocean color images in the La Plata continental shelf region, Continental Shelf Research, 28(13), 1568–1578, doi:10.1016/j.csr.2007.08.010, 2008.

Godad, S. P., Naidu, P. D. and Malmgren, B. A.: Sea surface temperature changes during May and August in the western Arabian Sea over the last 22 kyr : Implications as to shifting of the upwelling season, Marine Micropaleontology, 78(1-2), 25–29, doi:10.1016/j.marmicro.2010.09.006, 2011.

455   Gu, F., Zonneveld, K. A. F., Chiessi, C. M., Arz, H. W., Pätzold, J. and Behling, H.: Long-term vegetation, climate and ocean dynamics inferred from a 73,500 years old marine sediment core (GeoB2107-3) off southern Brazil, Quaternary Science Reviews, 172, 55–71, doi:10.1016/j.quascirev.2017.06.028, 2017.

Ito, R. G., Garcia, C. A. E. and Tavano, V. M.: Net sea-air CO_2 fluxes and modelled pCO_2 in the southwestern subtropical Atlantic continental shelf during spring 2010 and summer 2011, Continental Shelf
460   Research, 119, 68–84, doi:10.1016/J.CSR.2016.03.013, 2016.

Juggins. S., C2 Version 1.5 User guide. Software for ecological and palaeoecological data analysis and visualisation. Newcastle University, Newcastle upon Tyne, UK. 2007, 73pp.

Kucera, M., Rosell-Melé, A., Schneider, R., Waelbroeck, C. and Weinelt, M.: Multiproxy approach for the reconstruction of the glacial ocean surface (MARGO), Quaternary Science Reviews, 24(7-9), 813–819,
465   doi:10.1016/j.quascirev.2004.07.017, 2005a.

Kucera, M., Weinelt, M., Kiefer, T., Pflaumann, U., Hayes, A., Weinelt, M., Chen, M.-T., Mix, A. C., Barrows, T. T., Cortijo, E., Duprat, J., Juggins, S. and Waelbroeck, C.: Reconstruction of sea-surface temperatures from assemblages of planktonic foraminifera: multi-technique approach based on geographically constrained calibration data sets and its application to glacial Atlantic and Pacific Oceans,
470   Quaternary Science Reviews, 24(7-9), 951–998, doi:10.1016/j.quascirev.2004.07.014, 2005b.

Lantzsch, H., Hanebuth, T. J. J., Chiessi, C. M., Schwenk, T. and Violante, R. A.: The high-supply, current-dominated continental margin of southeastern South America during the late Quaternary, Quaternary Research, 81(02), 339–354, doi:10.1016/j.yqres.2014.01.003, 2014.

475   Lessa, D. V. de O., Portilho-Ramos, R. C., Barbosa, C. F., da Silva, A. R., Belem, A., Turcq, B., Albuquerque, A. L. and Ramos, R. P.: Planktonic foraminifera in the sediment of a western boundary upwelling system off Cabo Frio, Brazil, Marine Micropaleontology, 106, 55–68, doi:10.1016/j.marmicro.2013.12.003, 2014.

Lessa, D. V. O., Santos, T. P., Venancio, I. M. and Albuquerque, A. L. S.: Offshore expansion of the Brazilian coastal upwelling zones during Marine Isotope Stage 5, Global and Planetary Change,
480   158(September), 13–20, doi:10.1016/j.gloplacha.2017.09.006, 2017.

Lisiecki, L. E. and Stern, J. V.: Regional and global benthic Δ^{18}O stacks for the last glacial cycle, Paleoceanography, 31(10), 1368–1394, doi:10.1002/2016PA003002, 2016.

Locarnini R.A., Mishonov A.V., Antonov J.I., Boyer T.P., Garcia O.H.E., Baranova O.K., Zweng M.M.: World ocean database 2009, vol 1: temperature. US government printing office, Washington,DC., 2009.

485   Matsumoto, K., Chase, Z. and Kohfeld, K.: Different mechanisms of silicic acid leakage and their biogeochemical consequences, Paleoceanography, 29(3), 238–254, doi:10.1002/2013PA002588, 2014.

Mohtadi, M., Max, L., Hebbeln, D., Baumgart, A., Krück, N. and Jennerjahn, T.: Modern environmental conditions recorded in surface sediment samples off W and SW Indonesia: Planktonic foraminifera and biogenic compounds analyses, Marine Micropaleontology, 65(1-2), 96–112,
490   doi:10.1016/j.marmicro.2007.06.004, 2007.

Möller, O. O., Piola, A. R., Freitas, A. C. and Campos, E. J. D.: The effects of river discharge and seasonal winds on the shelf off southeastern South America, Continental Shelf Research, 28(13), 1607–1624, doi:10.1016/j.csr.2008.03.012, 2008.

Mortlock, R. A., Charles, C. D., Froelich, P. N., Zibello, M. A., Saltzman, J., Hays, J. D. and Burckle, L. H.:
495   Evidence for lower productivity in the Antarctic Ocean during the last glaciation, Nature, 351(6323), 220–223, doi:10.1038/351220a0, 1991.

Muller-Karger, F. E., Varela, R., Thunell, R., Luerssen, R., Hu, C. and Walsh, J. J.: The importance of continental margins in the global carbon cycle, Geophysical Research Letters, 32(1), 1–4, doi:10.1029/2004GL021346, 2005.

500   Paillard, D., Labeyrie, L. and Yiou, P.: Macintosh Program performs time-series analysis, Eos, Transactions American Geophysical Union, 77(39), 379, doi:10.1029/96EO00259, 1996.

Peeters, F., Brummer, G. and Ganssen, G.: stable isotope composition of *Globigerina bulloides* and *Globigerinoides ruber* (planktic foraminifera) in modern surface waters of the NW Arabian Sea, Global and Planetary Change, 34, 269–291, 10.1016/S0921-8181(02)00120-0, 2002.

505   Petró, S. M., Pivel, M. A. G., Coimbra, J. C. and Mizusaki, A. M. P.: Paleoceanographic changes through the last 130 ka in the western South Atlantic based on planktonic Foraminifera, Revista Brasileira de Paleontologia, 19(1), 3–14, doi:10.4072/rbp.2016.1.01, 2016.

Portilho-Ramos, R. C., Barbosa, C. F. and Rios-Netto, A. M.: Planktonic foraminiferal variations in the southwestern Atlantic since the last glacial-interglacial cycle, Palaios, 29(1), 38–44,
510   doi:10.2110/palo.2012.104, 2014a.

Portilho-Ramos, R. C., Ferreira, F., Lago, L. C., da Silva, A. G. V., Jaworski, K. S. and Toledo, M. B.: *Globorotalia crassaformis* optimum event: a new late Quaternary biostratigraphic marker for the southeastern Brazilian margin, Palaios, 29, 578–593, doi:10.2110/palo.2013.097, 2014b.

Portilho-Ramos, R. da C., Ferreira, F., Calado, L., Frontalini, F. and de Toledo, M. B.: Variability of the
515   upwelling system in the southeastern Brazilian margin for the last 110,000years, Global and Planetary Change, 135, 179–189, doi:10.1016/j.gloplacha.2015.11.003, 2015.

Rodrigues, R. R. and Lorenzzetti, J. A.: A numerical study of the effects of bottom topography and coastline geometry on the Southeast Brazilian coastal upwelling, Continental Shelf Research, 21(4), 371–394, doi:10.1016/S0278-4343(00)00094-7, 2001.

520   Rodrigues, S. V., Marinho, M. M., Cubas Jonck, C. C. C., Gonçalves, E. S., Brant, V. F., Paranhos, R., Curbelo, M. P. and Falcão, A. P.: Phytoplankton community structures in shelf and oceanic waters off southeast Brazil (20°-25°S), as determined by pigment signatures, Deep-Sea Research Part I: Oceanographic Research Papers, 88, 47–62, doi:10.1016/j.dsr.2014.03.006, 2014.

525   Santos, T. P., Lessa, D. O., Venancio, I. M., Chiessi, C. M., Mulitza, S., Kuhnert, H., Govin, A., Machado, T., Costa, K. B., Toledo, F., Dias, B. B. and Albuquerque, A. L. S.: Prolonged warming of the Brazil Current precedes deglaciations, Earth and Planetary Science Letters, 463, 1–12, doi:10.1016/j.epsl.2017.01.014, 2017.

Sarmiento, J. L., Gruber, N., Brzezinski, M. A. and Dunne, J. P.: High-latitude controls of thermocline nutrients and low latitude biological productivity., Nature, 427(6969), 56–60, doi:10.1038/nature10605, 2004.

530   Sautter, L. R. and Thunell, R. C.: Planktonic foraminiferal response to upwelling and seasonal hydrographic conditions; sediment trap results from San Pedro Basin, Southern California Bight, The Journal of Foraminiferal Research, 21(4), 347–363, doi:10.2113/gsjfr.21.4.347, 1991.

Schiebel, R. and Hemleben, C.: Ecology, in Planktic Foraminifers in the Modern Ocean, pp. 209–230, Springer Berlin Heidelberg, Berlin, Heidelberg., 2017.

535   Stainforth, R. M., Lamb, J. L., Luterbacher, H., Beard, J. H. and Jeffords, R. M.: Cenozoic Planktonic Foraminiferal Zonation and Characteristics of Index Formsle, The Paleontological Institute, The University of Kansas, Kansas. [online] Available from: http://hdl.handle.net/1808/3836 (Accessed 4 February 2015), 1975.

Stuiver, M. and Reimer, P. J.: Extended ^{14}C Data Base and Revised CALIB 3.0 ^{14}C Age Calibration Program, Radiocarbon, 35(1), 215–230, doi:10.1017/S0033822200013904, 1993.

540   Tessin, A. C. and Lund, D. C.: Isotopically depleted carbon in the mid-depth South Atlantic during the last deglaciation, Paleoceanography, 28(2), 296–306, doi:10.1002/palo.20026, 2013.

Thunell, R. and Sautter, L. R.: Planktonic foraminiferal faunal and stable isotopic indices of upwelling: a sediment trap study in the San Pedro Basin, Southern California Bight, Geological Society, London, Special Publications, 64(1), 77–91, doi:10.1144/GSL.SP.1992.064.01.05, 1992.

545   Toledo, F. A. L., Cachão, M., Costa, K. B. and Pivel, M. A. G.: Planktonic foraminifera, calcareous nannoplankton and ascidian variations during the last 25 kyr in the Southwestern Atlantic: A paleoproductivity signature?, Marine Micropaleontology, 64(1-2), 67–79, doi:10.1016/j.marmicro.2007.03.001, 2007.

Turner, J. T.: Zooplankton fecal pellets, marine snow, phytodetritus and the ocean's biological pump, Progress in Oceanography, 130, 205–248, doi:10.1016/j.pocean.2014.08.005, 2015.

550   Vargas, C. de, Bonzon, M., Rees, N. W., Pawlowski, J. and Zaninetti, L.: A molecular approach to biodiversity and biogeography in the planktonic foraminifer *Globigerinella siphonifera* (d'Orbigny), Marine Micropaleontology, 45(2), 101–116, doi:10.1016/S0377-8398(02)00037-3, 2002.

Volbers, A. N. A. and Henrich, R.: Calcium carbonate corrosiveness in the South Atlantic during the Last Glacial Maximum as inferred from changes in the preservation of *Globigerina bulloides*: A proxy to
555   determine deep-water circulation patterns?, Marine Geology, 204, 43–57, doi:10.1016/S0025-3227(03)00372-4, 2004.

Waelbroeck, C., Labeyrie, L., Michel, E., Duplessy, J. C., McManus, J. F., Lambeck, K., Balbon, E. and Labracherie, M.: Sea-level and deep water temperature changes derived from benthic foraminifera isotopic records, Quaternary Science Reviews, 21(1-3), 295–305, doi:10.1016/S0277-3791(01)00101-9, 2002.

560   Wang, D., Gouhier, T. C., Menge, B. A. and Ganguly, A. R.: Intensification and spatial homogenization of coastal upwelling under climate change, Nature, 518(7539), 390–394, doi:10.1038/nature14235, 2015.

Wang, X., Auler, A. S., Edwards, R. L., Cheng, H., Ito, E., Wang, Y., Kong, X. and Solheid, M.: Millennial-scale precipitation changes in southern Brazil over the past 90,000 years, Geophysical Research Letters, 34(23), L23701, doi:10.1029/2007GL031149, 2007.

565

Depth (cm)	14C age (yrs)	1 sigma error (yrs)	calendar age (cal ka BP)	1 sigma error (yrs)	notes	$\delta^{18}O$ points control	Reference
10	4140	80	4228	283			Tessin and Lund (2013)
18	6970	20	7463	201			Tessin and Lund (2013)
26	9895	25	10784	233			Tessin and Lund (2013)
30	10555	25	11795	298			Tessin and Lund (2013)
34	11955	30	13454	195			Tessin and Lund (2013)
38	12870	30	14550	341			Tessin and Lund (2013)
42	13650	35	16001	390			Tessin and Lund (2013)
50	4190	15	4281	264	reversal		Tessin and Lund (2013)
54	14080	35	16569	338			Tessin and Lund (2013)
56	10000	60	10967	147	reversal		Portilho-Ramos et al. (2014)
58	10990	35	12371	273	reversal		Tessin and Lund (2013)
60						15000	This study
66	10790	25	12091	273	reversal		Tessin and Lund (2013)
74	18010	100	20922	282			Tessin and Lund (2013)
82	16120	80	18994	199	reversal		Tessin and Lund (2013)
90	18100	60	20975	282			Tessin and Lund (2013)
98	19020	70	22074	292			Tessin and Lund (2013)
190	32550	270	37946	312			Portilho-Ramos et al. (2014)
260						63400	This study
350						70000	This study

Table 1: Chronology of core JPC-17 obtained by accelerator mass spectrometry (AMS ^{14}C) dating on

planktonic foraminifera shells (Tessin and Lund, 2013; Portilho-Ramos et al., 2014a) and stable isotope ($\delta^{18}O$)

tie-points tuned to stack LS16 from Lisiecki and Stern (2016)

570
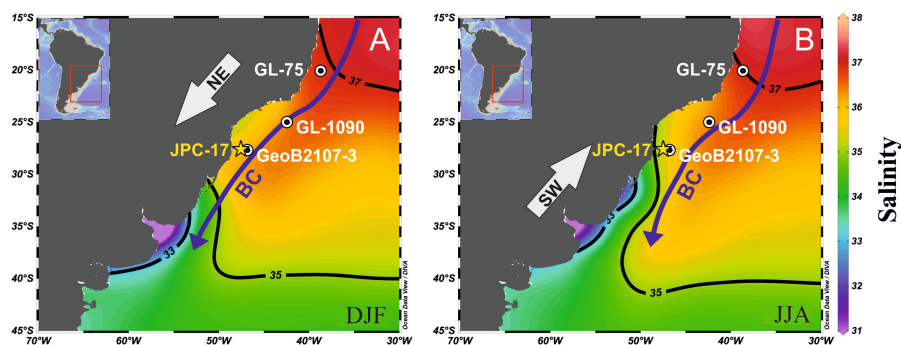
Figure 1: Surface salinity in southwestern Atlantic Ocean (Locarnini et al., 2010) during (**A**) austral summer (December-February, DJF) and (**B**) winter (June-August, JJA) showing the location of cores JPC-17 (this study), GeoB2107-3 (27°17'S; 46°45'W; Gu et al., 2017), GL-1090 (24°92'S; 42°51' W; Santos et al., 2017) and GL-75 (Portilho-Ramos et al., 2015). Blue arrows indicate the western boundary Brazil Current (BC) and the gray arrows show the regional prevailing alongshore wind direction (northeastern – NE and southwestern – SW). Figure created using the Ocean Data View software (ODV - version, 4.7.10., http://odv.awi.de, 2018).
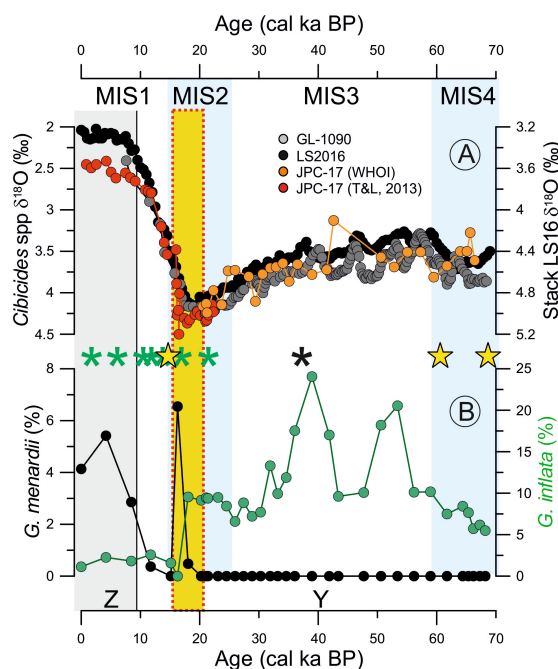
Figure 2: Age model of core JPC-17. (**A**) Comparison between the benthic foraminifera δ¹⁸O record of JPC-17 (composed of published *Cibicidoides* spp. (Tessin and Lund, 2013; T&L, 2013) and unpublished *Cibicidoides* spp. data from Woods Hole Oceanographic Institution - WHOI) to the benthic foraminifera δ¹⁸O record of core GL-1090 (Santos et al., 2017) as well as to the intermediate-depth South Atlantic benthic δ¹⁸O stack LS16 (Lisiecki and Stern, 2016). Asterisks represent the calibrated radiocarbon ages published in (green) Tessin and Lund (2013) and (black) Portilho-Ramos et al. (2014), while yellow stars represent the δ¹⁸O tie-points shown in Table 2. (**B**). Abundance of the main biostratigraphical planktonic foraminifera species *Globorotalia menardii* and *Globorotalia inflata* from core JPC-17. Marine Isotopic Stages 1 to 4 (MIS1–4; MIS 2 and 4 indicated by vertical blue bars) are shown at the top, while letters Z (vertical grey bar) and Y in the bottom correspond to biostratigraphical biozones of Ericson and Wollin (1968). The vertical yellow bar marks the interval with reversed radiocarbon ages listed in Table 1.
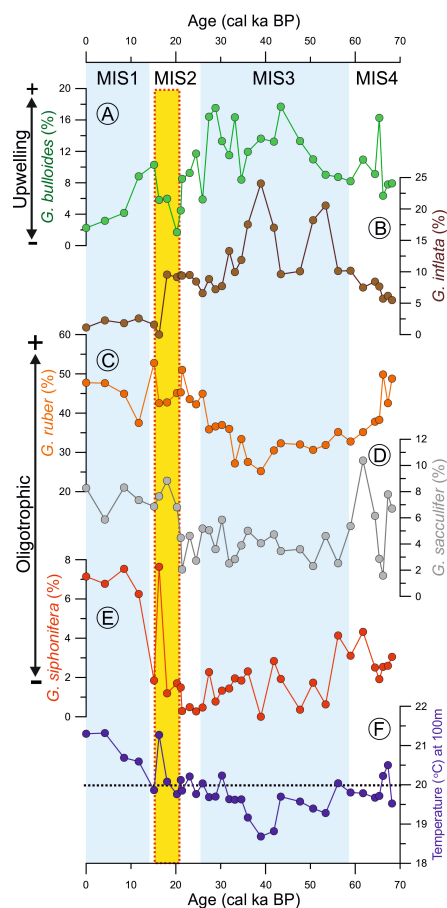
Figure 3: Relative abundance of planktonic foraminifera species and reconstructed subsurface temperature (100 m water depth) from core JPC-17 over the last 70 kyr. (**A**) Relative abundance of *Globigerina bulloides*, (**B**) *Globorotalia inflata*, (**C**) *Globigerinoides ruber*, (**D**) *Glogigerinoides sacculifer* and (**E**) *Globigerinella siphonifera*. (**F**) Temperature at 100m water depth. Blue dashed line in (**F**) indicates the 20°C isotherm which defines the modern maximum temperature of South Atlantic Central Water (Castelao et al., 2004), the water mass entering the photic zone in the upwelling sites of the southern Brazilian margin. The vertical yellow bar marks the interval with reversed radiocarbon ages listed in Table 1.
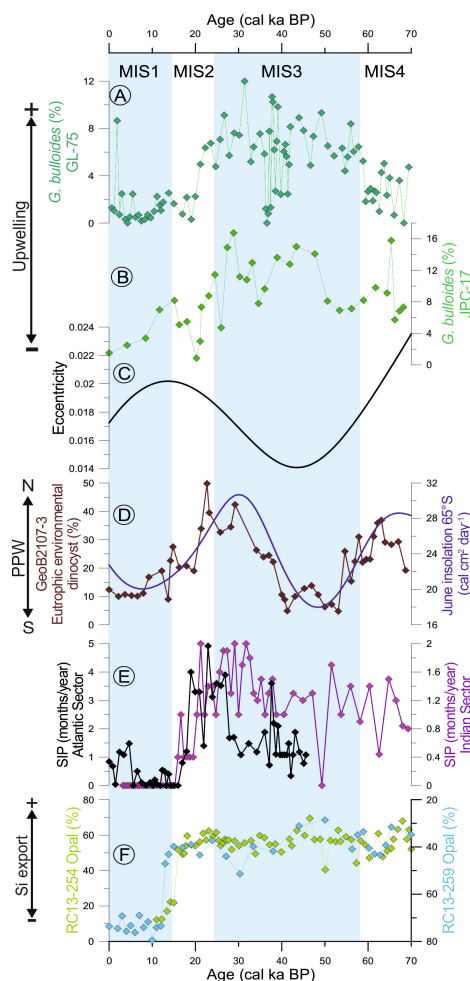
Figure 4: Mechanism behind the variability of the productivity in the southern Brazilian margin over the last 70 kyr. Abundance of upwelling indicator species *G. bulloides* from (**A**) core GL-75 (21°S) (Portilho-Ramos et al., 2015) and (**B**) core JPC-17 (27°S) (this study). **C.** Eccentricity and austral summer (January) insolation at 15°S (Berger and Loutre, 1991). **D.** Abundance of dinoflagellate cysts from core GeoB 2107-3 (27°S) representing the influence of the Plata Plume Water in the southern Brazilian margin (Gu et al., 2017) and austral winter (June) insolation at 65°S (Berger and Loutre, 1991). **E.** Antarctic sea ice presence (SIP) in the Atlantic Sector core TN057-13-PC4 (53°20′S; 5°10'W; Shemesh et al 2002) and Indian Sector core SO136-111 (56°40'S; 160°14'W; Crosta et al., 2004) sectors of the Southern Ocean derived from diatoms assemblage. **F.** Opal content in Atlantic sector of the Southern Ocean cores RC13-254 (48°34′S; 5°34′E) and core RC13-259 (53°53′S; 4°56'W) as a proxy for silicic acid transport toward low latitudes (Mortlock et al., 1991). Core RC13-254 is located to the north of the Antarctic Polar Zone (APZ) while core RC13-254 is located to the south of the APZ. Note the inverted (RC13-259) axis in (**F**).